Available online at www.sciencedirect.com
ScienceDirect
Journal of Power Sources 161 (2006) 1400–1411
JOURNAL OF POWER SOURCES
www.elsevier.com/locate/jpowsour

Dynamic model of a lead acid battery for use in a domestic fuel cell system

Matthias Dürr*, Andrew Cruden, Sinclair Gair, J.R. McDonald

Centre for Economic Renewable Power Delivery, University of Strathclyde, 204 George Street, Glasgow G1 1XW, United Kingdom

Received 2 February 2005; received in revised form 25 October 2005; accepted 21 December 2005
Available online 8 February 2006

Abstract

This paper presents a review of existing dynamic electrical battery models and subsequently describes a new mathematical model of a lead acid battery, using a non-linear function for the maximum available energy related to the battery discharge rate. The battery state of charge (SOC) is expressed in a look-up table relative to the battery open circuit voltage (VOC). This look-up table has been developed through low discharge experiments of the battery modelled. Further, both the internal resistance and self-discharge resistance of the battery are subsequently expressed as functions of the open circuit voltage. By using an electrical model with these characteristics and a temperature compensation element to model different rates of charge and discharge, a relatively simple and accurate battery model has been developed.

The new model takes into account battery storage capacity, internal resistance, self-discharge resistance, the electric losses and the temperature dependence of a lead acid battery. It is shown in this paper how the necessary parameters for the model were found. The battery modelled was a Hawker Genesis 42 Ah rated gelled lead acid battery.

The simulation results of the new model are compared with test data recorded from battery discharge tests, which validate the accuracy of the new model.

Keywords: Dynamic model; Lead acid; Battery

1. Introduction

This paper forms the first part of a series of papers describing, modelling and testing a complete domestic scale fuel cell (FC) combined heat and power (CHP) system. This FC CHP system, built at the University of Strathclyde, has been described in detail in [1]. The motivation to develop a new battery model within the Matlab/Simulink environment lies in the study of a domestic scale fuel cell system, in which a lead acid battery bank is used as an energy storage/buffer device. To simulate and study the overall FC system the behaviour of each element, in this first case the lead acid battery, has to be fully understood and models short term discharge performance before going on in a separate paper to investigate long term cycling effects.

Most of the commercial research in stationary FC technology is concentrated in the development of grid-connected systems, which typically do not have integrated thermal and electric buffer/storage systems [2]. This is mainly due to cost reasons, as the control system will be less complicated and therefore less expensive, the costs for the buffer devices will be avoided and operation and maintenance costs (O&M costs) will be reduced. Any additional electrical power, e.g. for fast or peak load changes, will be drawn from the electrical grid for such a system. That kind of system configuration is primarily suitable for integration in infrastructures with an existing electrical grid connection, hence, mainly in urban areas. The FC system is electric power controlled, which makes it necessary to match electrical supply and demand powers at all times. Due to cost concerns it is more economic to use a hybrid FC/battery system than purely a FC only system.

The advantages of a hybrid FC/battery system for a grid independent system can be easily understood by analysing a typical domestic load profile (Fig. 1).

* Corresponding author.
E-mail address: m.duerr@eee.strath.ac.uk (M. Dürr).

0378-7753/$ – see front matter © 2006 Elsevier B.V. All rights reserved.
doi:10.1016/j.jpowsour.2005.12.075

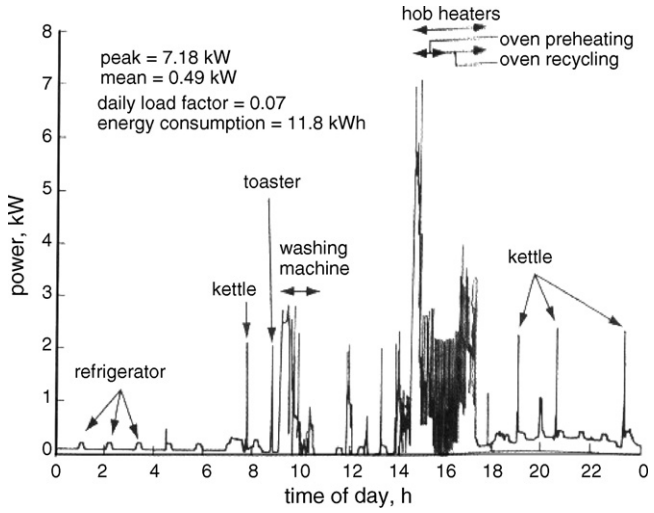

Fig. 1. Typical single household load profile in the UK, summer period [3].

A domestic electric load profile of a typical single household in the UK (summer period) gives an average power demand of 0.5 kW_e, but a peak power demand of greater than 7 kW_e. This profile is assumed constant throughout the year, as thermal demand is anticipated to be met through an existing central heating system. With FC prices currently between £1500 kW_e^{-1} and £5000 kW_e^{-1}, FC stacks remain far more expensive than battery systems (£70–300 kWh^{-1}); hence, it makes economic sense to use a FC with a rating of approximately the average power demand to allow a relatively high running time of the FC [4–6]. The additional power is provided by a backup system (e.g. batteries).

The FC system developed at Strathclyde University uses an alkaline fuel cell (AFC) that has a current increase limitation of 10 A s^{-1}, which makes it necessary to provide additional power for sudden load demands from batteries.

Mainly for cost reasons (e.g. see Fig. 4) the FC/battery hybrid system will use lead acid batteries and in particular gel-filled Hawker Genesis 12 V dc 42 Ah types to minimise the safety risk of acid leakage within an fuel cell system environment. Nonetheless, the model described here can be used for other battery types by changing the energy–voltage characteristic and the internal model parameters as introduced later. In the following sections, the experimental tests used to determine these parameters with a simple battery test station are described followed by a detailed presentation of the battery model developed.

1.1. Lead acid batteries

Lead acid batteries are still the most common devices to store and deliver electricity in the range from 5 V to 24 V dc [7]. A low price, high availability and ease of manufacture account for the wide use of the lead acid battery in many designs, sizes, and system voltages. The lead acid battery is almost always the least expensive storage battery for any application, while still providing reasonable performance and life characteristics. Fig. 2 gives a comparison of main characteristics for commonly used types of secondary batteries. The numbers 1–5 give a rating from 1—excellent to 5—poor performance.

During the mid 1970s the design of the lead acid battery has been improved by the development of the maintenance-free lead acid battery that could operate in any position. The liquid electrolyte was transformed into moistened separators and the enclosure was sealed. Safety valves were added to allow venting of gas during charge and discharge. Driven by different market needs, two lead acid systems emerged: the sealed lead acid (SLA), also known under the brand name of Gelcell, and the valve-regulated lead acid (VRLA).

System	Energy Density	Power density	Discharge profile	Cycle Life	Cost
Lead-Acid	4 (34.7Wh/kg)*	3 (75-130W/kg)	3 flat	400 **	1 £80/kWh
Lithium-Ion	2 (90Wh/kg)	3	4 sloping	500-1000	3
Nickel-Cadmium	5 (30Wh/kg)	2 (150-200W/kg)	1 very flat	500-2000	3 £400/kWh
Nickel-Iron	5 (27Wh/kg)	2	3 moderately flat	2000-4000	3
Nickel-metal hydride	3 (50Wh/kg)	2 (120-250W/kg)	2 flat	300-600	3 £360/kWh
Nickel-Zinc	2 (60Wh/kg)	5	2 flat	50-200	3
Nickel-hydrogen	1 (100Wh/kg)	1 (400W/kg)	3 moderately flat	1500-6000	5 approx. £2500/kWh
Zinc-Manganese dioxide	2 (80Wh/kg)	3	5 sloping	15-25	2

Fig. 2. Comparison of different secondary batteries [8,10]. (*) Hawker Genesis 42 Ah at C_{10} discharge rate [9]. (**) Hawker Genesis at 100% depth of discharge [9].

2. Battery models

As mentioned before, it is very difficult to develop a truly generic model, which takes all factors of a battery into account. Depending on the use of the model different approaches have been made.

In the following section some of the most common electrical circuit battery models are introduced and their main features are explained.

2.1. Simple model

The most simple and commonly used model of a battery consists of a constant resistance R_b in series with an ideal voltage source E_0 [e.g. 11]. The open circuit voltage VOC gives the voltage across the ideal battery, whereas the voltage across the ideal battery and resistance R_b gives the terminal voltage of the battery V_b.

This simple model does not take into account the true internal resistance of the battery, which is highly related to the state of charge and the electrolyte concentration. In this case, the energy drawn can be unlimited. This model is only suitable for applications where the state of charge is not important, i.e. very simplistic modelling.

2.2. Improved simple model

To take recognition of the role of the state of charge this battery model varies the resistance of the battery, i.e. R_b is now a function of the state of charge (SOC). The block diagram is the same as for the simple model in Fig. 3 with the only difference that R_b is variable resistor depending on the state of charge. A typical equation for R_b is:

$$R_b = \frac{R_o}{S^k} \tag{1}$$

where

$$S = 1 - \frac{Ah}{C_{10}} \tag{2}$$

C_{10} is the 10-h capacity (Ah) at a reference temperature, A the discharge current (A), h the time of discharging (h), R_o the resistance of the fully charged battery (Ω), S the state of charge factor, and k is the capacity coefficient.

S varies from 0, for fully discharged up to 1, for fully charged. The coefficient k in the improved simple model takes the change in battery capacity under different discharge rates into account,

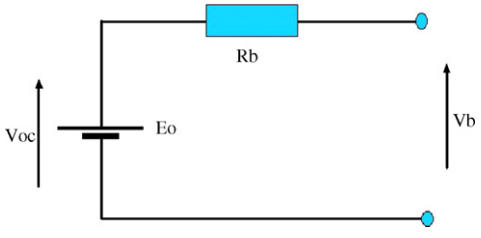

Fig. 3. Simple battery model.

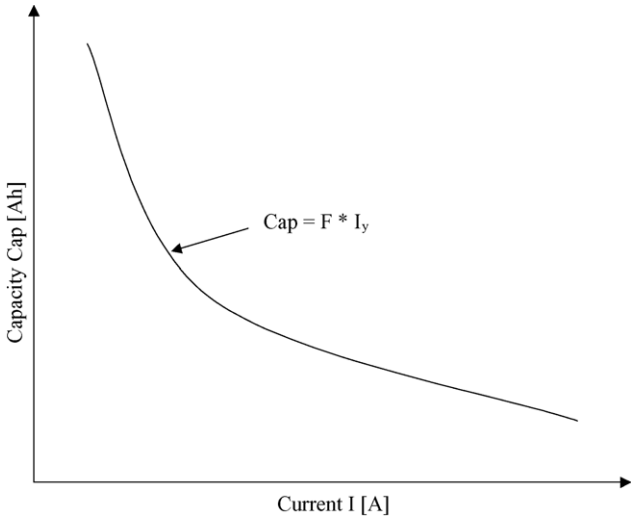

Fig. 4. Battery capacity vs. discharge rate.

similar to the so-called Peukert factor [12]. The Peukert equation gives a simple empirical relationship between the battery capacity and the discharge range, shown in Fig. 4.

The relationship can be written in the form of:

$$\text{Cap} = F \times I^y \tag{3}$$

with Cap the battery capacity (Ah), I the discharge current (A), F the constant factor (h), y the constant exponential factor (Peukert factor).

2.3. Thevenin battery model

The other common basic battery model describes a battery with an ideal battery voltage (E_0), internal resistance (R), a capacitance (C_o), and an over-voltage resistance (R_o) [13–15]. C_o represents the actual capacitance of the battery, the so-called double layer capacitance, and the resistor R_o represents the resistance contributed by the contact resistance of the plates and the electrolyte. The main disadvantage of this model is that all the components are constant, whereas in reality all these characteristics vary dependent on the state of charge (SOC) and the discharge rate. Especially there is no recognition in the model of the battery electrochemistry, the so-called Faradaic process, and the resulting limitations from it.

2.4. Non-linear dynamic battery model

A more realistic dynamic battery model has been created by expanding the Thevenin model, to take account of the non-linear parameters [15,16]. The internal resistance, self-discharge resistance and overcharge resistance are characterised and the charging and discharging processes of the battery are separated (Fig. 5).

The values of these elements are functions of the open circuit voltage of the battery, which in turn is an indirect expression of the state of charge of the battery. The model is pictured in Fig. 6.

The elements involved in this model can be described as follows:

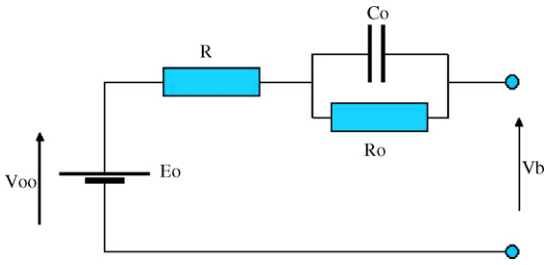

Fig. 5. Thevenin battery model.

- C_b – battery capacitance – the battery is an electrical storage device, which is considered equivalent to a capacitor. The SOC therefore is described in terms of the amount of stored charge. The capacitance C_b of the battery can be modelled as a controlled voltage source within Matlab, which is controlled relative to the state of charge of the battery.
- R_p – self-discharge resistance – R_p takes into account that the battery has a small self-discharge leakage current which is a function of the open circuit voltage.
- R_{ic} and R_{id} – internal resistance – R_{ic} and R_{id} take the resistance of the electrolyte and the resistance of the battery plates into account. These resistances are different between the charge and discharge processes.
- R_{co}, R_{do}, and C_o – the voltage drop at switch on in a lead acid battery cannot be represented solely by the contribution of the internal resistance. In fact, the overpotential is the most important factor in the voltage drop. The overpotential is caused by mass transport and activation limitations on the cathode and anode of the battery. In an electrical circuit model, this drop can be expressed with a parallel *R–C* branch. The voltage drop for the charge and discharge process is represented by R_{co} and R_{do}, whereas C_o represents the double layer capacitance behaviour of the battery during charge and discharge.

This model takes into account the variation of the elements with the open circuit voltage VOC, taken from measurement and/or data sheets. This data is used to create functions of the capacity and resistances of the battery relative to the open circuit voltage, and hence the model behaves more accurately. The voltage dependent capacitance curve has been determined by curve fitting to sets of experimental data as [7]:

$$C = k \times e^{(W \times (V_m - \mathrm{VOC}))^F} \quad (4)$$

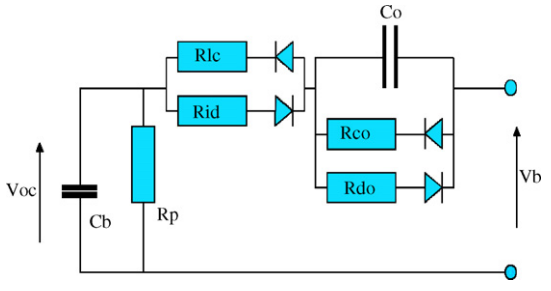

Fig. 6. Dynamic battery model.

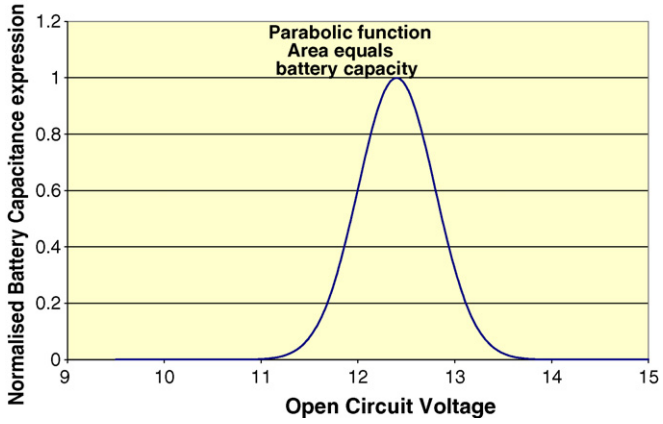

Fig. 7. Capacitance–open circuit voltage characteristic.

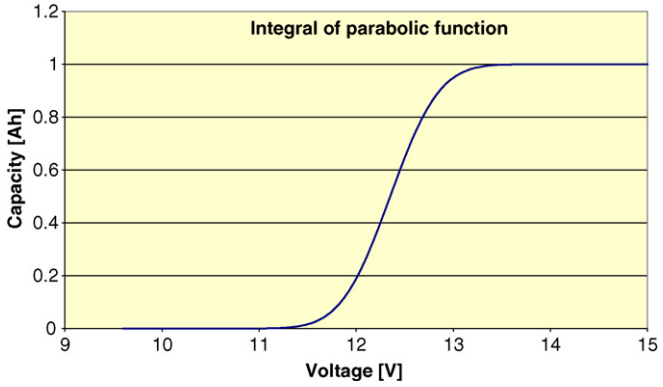

Fig. 8. Capacity–open circuit voltage characteristic (integration of Fig. 9).

with *C* the battery element modelled, capacitance (F), *k* the constant (gain factor), *W* the width factor (negative value), V_m the mean voltage (in this model 12.4 V), VOC the open circuit voltage, and *F* is the flatness factor (set to 2).

This parabolic battery capacitance function/curve is centred about the open circuit voltage of the fully charged battery. *F* was chosen to be equal to 2, which gives a parabolic function. By varying the negative factor *W* the curve was chosen such that the area under the curve was equal to unity, therefore enabling the coefficient *k* to be fit to the manufacturers stated battery capacity. The parabolic curve is pictured in Fig. 7 and the integral of this function is given in Fig. 8.

Similar functions are used in other model approaches (e.g. Advisor battery model [17]) to estimate the relationship between open circuit voltage and energy state of charge of the battery.

3. A new approach to a dynamic battery computer model

Recognising that many factors influence battery behaviour and that there are difficulties in describing them accurately and simply in a dynamic, non-linear model, a new approach to battery modelling is presented. Based on the non-linear battery model in Section 2.4 the author's model uses a new approach to determine the open circuit voltage during a dynamic simulation. In the new model, the open circuit voltage VOC depends

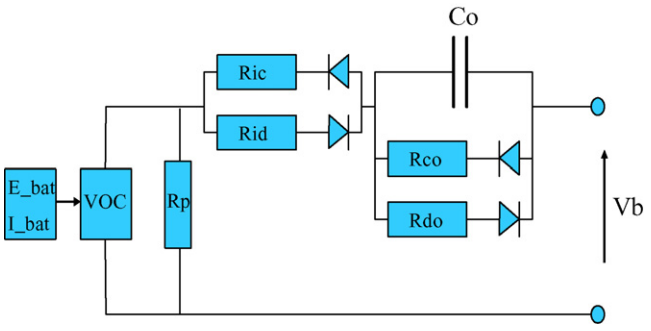

Fig. 9. New dynamic battery model.

on the actual discharge current I_B, the energy drawn from the battery E_{cd} and the battery temperature T. All model parameters are non-linear and are described using mathematical functions.

A schematic of the proposed model is shown in Fig. 9. The model was implemented in Matlab/Simulink and uses elements from the Power System Blockset.

The dynamic model described in Section 2.4 demonstrates good correlation with experimental results; however, the battery is not an ideal capacitor, which makes the model inaccurate for different discharge rates. The drawback of this model is that the equation used to determine the capacity of the battery can only be an approximation of the real battery capacity and the accuracy of the used mathematical function representing the battery capacity. Further the capacitance is modelled as a complicated mathematical function using various mathematical parameters, which complicates the battery model (see Fig. 7 and Eq. (4)).

The author's model develops a new simple approach relating the calculated remaining energy of the battery to the open circuit voltage using a look-up table, which is based on discharge tests at low discharge rates. A block diagram of the algorithm to determine the open circuit voltage VOC is given in Fig. 10.

This model uses the initial battery current I_B, when connected to a load, to predict the maximum available energy at a given temperature. Hence, different rates of discharge at different temperatures can be accurately modelled. The energy being drawn from the battery is dynamically calculated and subtracted from the initial energy to give a value of remaining battery energy and state of charge (SOC). Knowing the remaining battery energy allows a new value for the battery open circuit voltage to be determined using the look-up table.

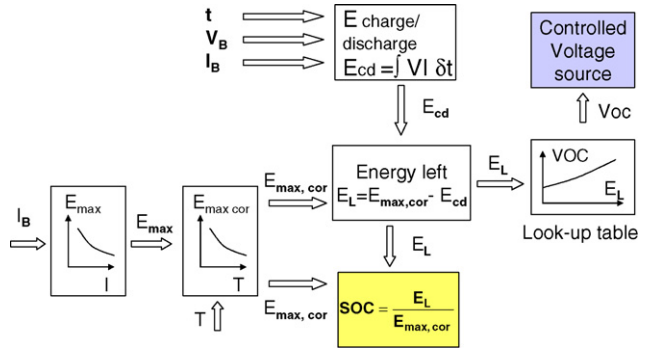

Fig. 10. Algorithm to determine open circuit voltage of the battery model.

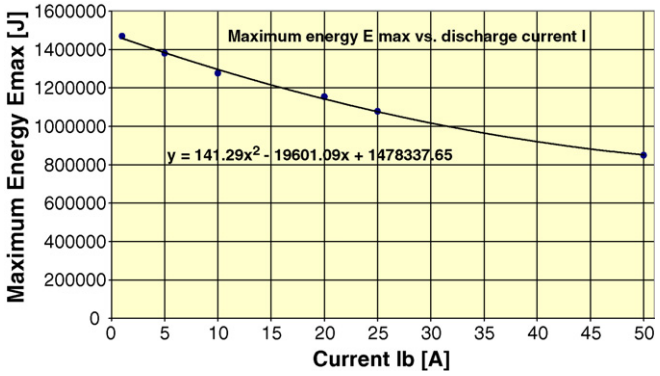

Fig. 11. Constant discharge current I_B vs. maximum energy.

Several discharge tests at different constant current rates have been carried out and the results have been used to determine a simple function to describe the relationship between discharge rate and maximum available energy accurately.

The test results for the modelled 42 Ah Hawker Genesis battery and the curve that represents this data is shown in Fig. 11.

The function was defined as:

$$E_{max} = 141.29 \times I_B^2 - 19601 \times I_B + 1.478 \times 10^6 \quad (5)$$

At each time step of the simulation the energy drawn from the battery is calculated with the equation:

$$E_{cd} = \int V_b I_B \, \delta t \quad (6)$$

with E_{cd} the energy drawn from battery (J), V_b the battery terminal voltage (V), I_B the battery current (A), and t the time (s).

The model assumes that the simulation starts with a fully charged battery, hence, the initial energy of the battery equals E_{max}. For each time step of the simulation the remaining battery energy E_L is defined as:

$$E_L = E_{max} - E_{cd} \quad (7)$$

Consequently, the battery state of charge SOC can be dynamically expressed as the quotient of remaining energy E_L and maximum energy E_{max}:

$$SOC = \frac{E_L}{E_{max}} \quad (8)$$

3.1. The energy versus open circuit voltage look-up table

The remaining energy E_L versus open circuit voltage (VOC) characteristic is implemented using experimental data derived from a low discharge rate test. Experiments have shown that the open circuit voltage VOC for a fully charged battery is given as 12.81 V with a related battery energy of 1.5×10^6 J. Fully discharged the battery open circuit voltage drops to 11.58 V and the remaining energy E_L equals zero.

The characteristic shown in Fig. 12 has been implemented in the model as a look-up table with the input variable as remaining energy E_L and the output variable as open circuit voltage (VOC).

A low rate constant discharge test has been carried out and the energy drawn from the battery E_{cd} has been calculated using

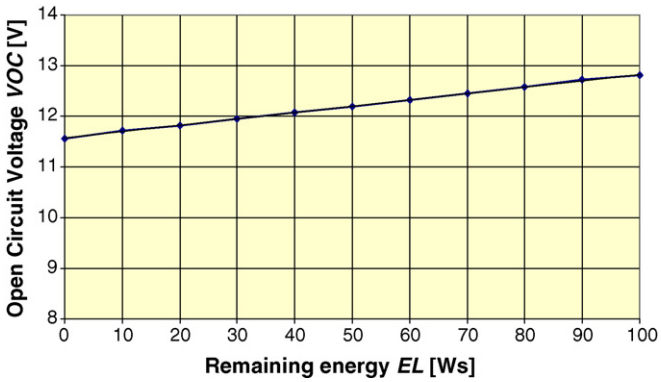

Fig. 12. Battery remaining energy E_L vs. open circuit voltage.

Eq. (6). The maximum energy E_{max} is known for the chosen discharge rate for the tested discharge and has been used to calculate the remaining energy E_L with Eq. (7).

The energy–VOC look-up table has been generated from experimental results. Using the described battery discharge station a constant low rate discharge test has been carried out. The discharge time t, the current I_B and the battery terminal voltage V_b have been recorded. This information allows calculating the remaining battery energy E_L. The test station has been programmed to disconnect the load after a specified discharge time Δt. The battery voltage recovers and stabilise at the open circuit voltage VOC. The measured VOC is related to the calculated battery energy E_L for the specified discharge time. The procedure has been repeated till the battery has been fully discharged and an energy/VOC look-up table has been generated. A typical discharge pattern for this test is shown in Fig. 13.

3.2. Internal resistance for charge and discharge of the battery

The internal resistance, R_i, will vary over the voltage range of the battery and is dependent on the direction of current flow (charge or discharge).

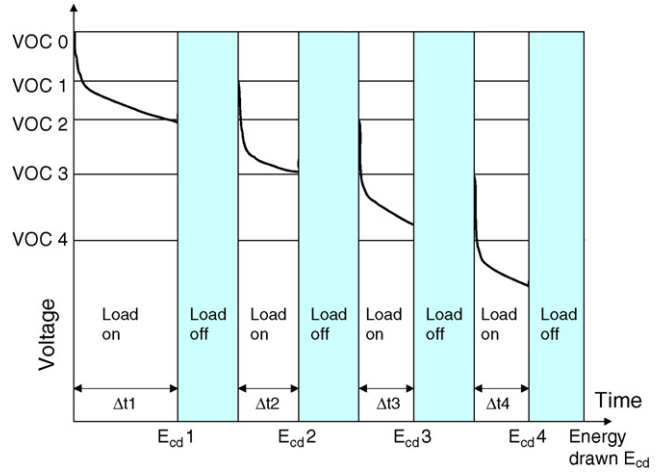

Fig. 13. Discharge pattern.

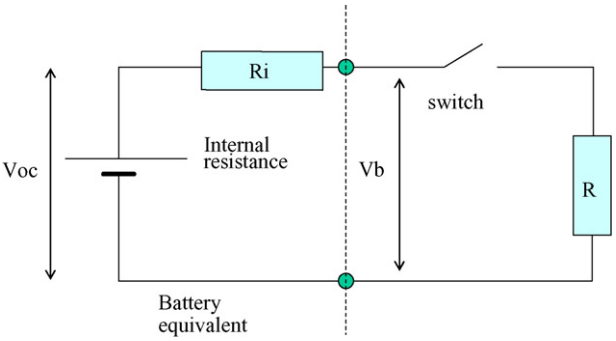

Fig. 14. Circuit diagram internal resistance test.

To determine these parameters, a resistor was connected to the battery as shown in Fig. 14.

By opening and closing the switch two different values of voltage can be can measured at the battery terminals; with the switch open the open circuit voltage VOC is measured and with the switch closed the battery voltage V_b is measured. The electric circuit equation is given below:

$$V_b = \mathrm{VOC}\frac{R}{R_i + R} \tag{9}$$

Hence, the internal resistance can be expressed with:

$$R_i = R\frac{(\mathrm{VOC} - V_b)}{V_b} \tag{10}$$

Measuring the voltage VOC and V_b at different states of charge leads to the curves presented in Figs. 15 and 16.

The transient that occurs during switching between two different load levels can be used to determine the capacitance of the battery discussed in Section 3.4.

The internal resistors for charge and discharge cycles are modelled as series resistances. They are modelled in Simulink using controlled voltage sources.

3.3. Self-discharge resistance of the battery

The self-discharge phenomenon of lead acid batteries is due to the fact that the electrode reactions are normally in favour of the discharge reaction, which means thermodynamically the

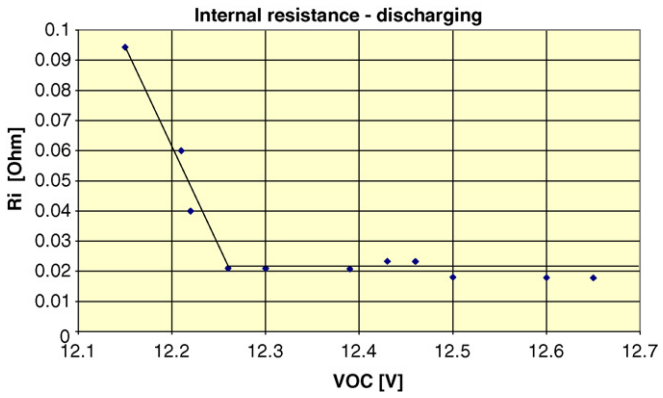

Fig. 15. Internal resistance during discharging, R_{id}.

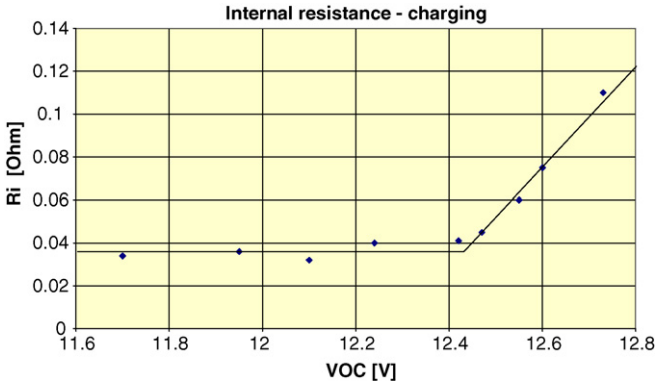

Fig. 16. Internal resistance during charging, R_{ic}.

discharged state is the most stable [8]. Lead and lead dioxide are unstable in sulphuric acid, and on open circuit, they react with the electrolyte. These reactions generate oxygen on the positive electrode (Eq. (11)) and hydrogen on the negative electrode (Eq. (12)).

$$PbO_2 + H_2SO_4 \rightarrow PbSO_4 + H_2O + 0.5O_2 \quad (11)$$

$$Pb + H_2SO_4 \rightarrow PbSO_4 + H_2 \quad (12)$$

These chemical reactions typically cause the self-discharge of a lead acid battery [8].

The self-discharge resistance R_p, is modelled in the same fashion as the other non-linear resistances dependent on VOC, e.g. shown in Section 2.4. By knowing the state of charge versus open circuit voltage characteristic of a battery the self-discharge resistance can be estimated for different states of charge.

The battery voltage of the modelled Hawker Genesis battery was recorded over a period of 6 months. Fig. 17 shows the measured drop in battery VOC caused by the self-discharge phenomenon for this test.

The open circuit voltage is related to a characteristic energy level (e.g. Fig. 13). By monitoring the gradual voltage drop of an isolated battery over a long period (typically 2–6 months) the energy losses can be deduced via the E_{max} versus VOC characteristic (Fig. 11). The author assumes that the self-discharge current is nearly zero, which leads to a maximum battery energy E_{max} of 1.478 MJ. The energy loss relative to the maximum battery energy can then be calculated.

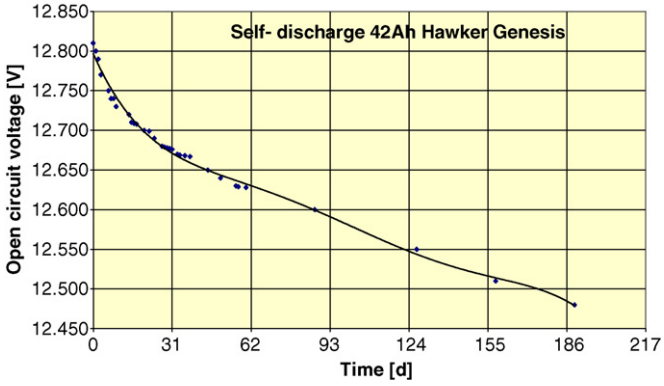

Fig. 17. Open circuit voltage drop caused by self-discharge.

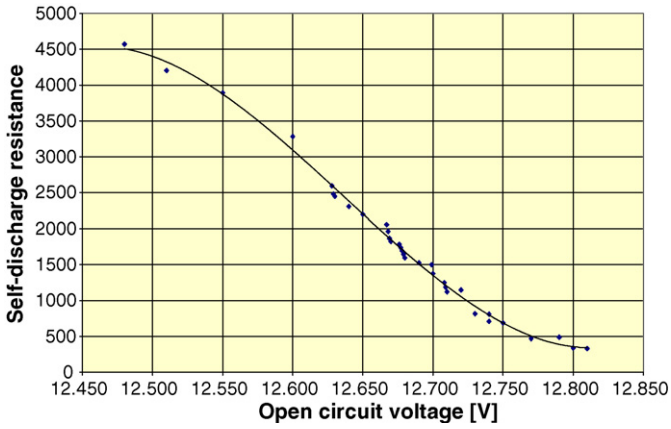

Fig. 18. Self-discharge resistance related to open circuit voltage.

$$\Delta E = E_{max}(1 - SOC) \quad (13)$$

The average self-discharge current flow can be expressed using:

$$I = \frac{\Delta E}{VOC \times t} \quad (14)$$

This leads to the self-discharge resistance:

$$R_p = \frac{VOC}{I} \quad (15)$$

where R_p is the self-discharge resistance of the battery (Ω), I the current caused by self-discharged (A), E_{max} the maximum battery energy (J), ΔE the battery energy during the self-discharge test (J), t the time data of self-discharge test (s), VOC the average open circuit voltage between two points of the self-discharge test (V), and SOC is the battery state of charge.

The self-discharge resistance derived, relative to the open circuit voltage, is illustrated in Fig. 18 and implemented in the dynamic battery model.

3.4. Faradaic resistance and double layer capacitance elements

The parallel resistor R_o–capacitor C_o branch is implemented in the electrical circuit model to take into account the double layer capacitance of the battery and the voltage drop caused by the electrode kinetics and the Faradaic process under load conditions. Especially activation losses at low load current and mass transport losses at higher current reduce the ideal battery terminal voltage.

A parallel capacitor–resistor (R_o–C_o) network models this behaviour during charging and discharging of the battery. R_o is part of the internal resistance and are included in the values given in Figs. 15 and 16. The double layer capacitance C_o was determined through tests, recording the voltage transient behaviour of the battery during switching between two different load levels R_1 and $R_1 + R_2$. The experimental set-up is pictured in Fig. 19.

The voltage response was recorded using a digital storage oscilloscope and the time constant τ was determined (Fig. 20).

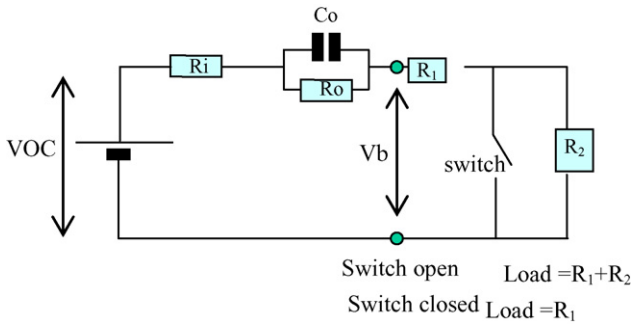

Fig. 19. Test set-up to determine the battery double layer capacitance.

The capacitance was than calculated using Eq. (16).

$$C_o = \frac{\tau}{R_c} \tag{16}$$

R_c represents the resistance of the battery circuit (R_i, R_o) connected to the load (R_1) and has been calculated to:

$$R_c = \frac{R_o \times (R_i + R_1)}{R_o + (R_i + R_1)} \tag{17}$$

C_o has been calculated to 250 mF for the investigated Hawker Genesis battery.

3.5. Temperature effects on the battery performance

The temperature at which the battery is discharged has an important effect on its available capacity and hence voltage characteristic. This is due to the reduction in chemical activity and the increase in battery internal resistance at lower temperatures [8]. Lowering the temperature will result in a reduction of capacity as well as an increase in the slope of the discharge curve (Fig. 21). The performance will vary for different battery systems, but in general the optimum performance is obtained between 15 °C and 25 °C. At higher temperatures, chemical deterioration of the battery plates and electrolyte may be rapid enough during discharge to cause a loss in capacity and over a longer period would severely reduce the lifetime of the battery due to positive grid corrosion.

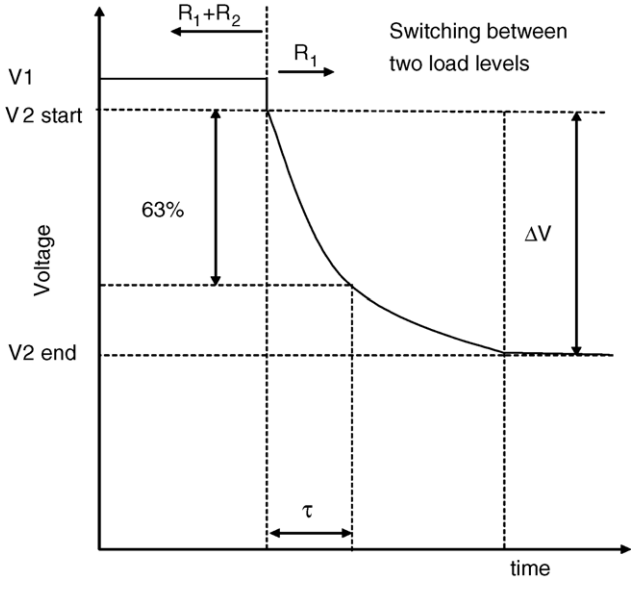

Fig. 20. Experimental determination of time constant τ.

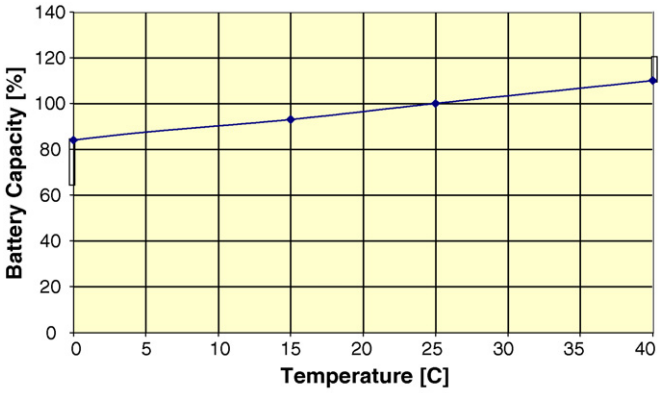

Temperature [°C]	0	15	25	40
Capacity at 15min rate [%]	84	93	100	110

Fig. 21. Battery capacity vs. temperature characteristic for Hawker Genesis [18].

However, to be able to model the battery behaviour at lower and higher temperatures, temperatures between 0 °C and 40 °C have been taken into account for the model.

As expected, laboratory tests have shown that the capacity of the battery decreases at lower temperatures, implying the battery capacity is temperature dependent. Different approaches to implement thermal effects in battery models are suggested in Refs. [12,15,19].

In the author's model the maximum battery capacity has been adjusted for temperature, as shown in Fig. 21, by using manufacturer's data [9,18]. As suggested from the battery manufacturer the author's model uses a function, which describes the capacity–temperature characteristic. The empirical function of this compensation factor F_{Temp} has the following form:

$$F_{Temp} = \frac{-0.002T^2 + 0.793T + 82.42}{100} \tag{18}$$

with T the battery temperature (°C) and F_{Temp} the compensation factor.

The temperature corrected maximum energy $E_{max,corr}$ is defined as the product of the compensation factor F_{Temp} and the nominal maximum energy E_{max}, which is given at 25 °C.

$$E_{max,corr} = F_{Temp} \times E_{max} \tag{19}$$

4. Discharge tests

To verify the simulation results it was necessary to carry out a range of tests using a 42 Ah Hawker Genesis battery. For this purpose a test station was built, consisting of an electronic load (model: Emerson Electronic load EL-300), measurement equipment for voltage, current and temperature and a computer

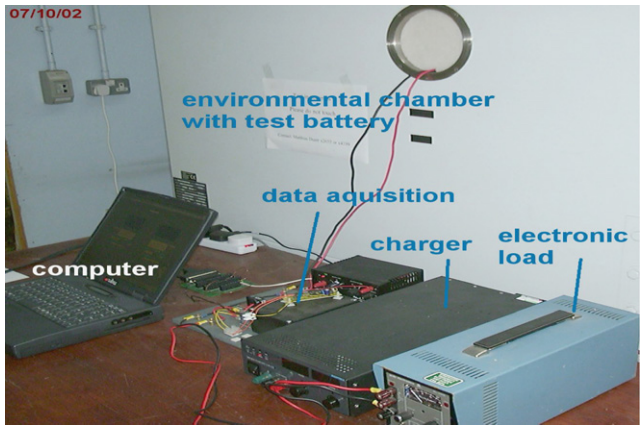

Fig. 22. Battery test station.

data acquisition system. Furthermore an environmental chamber (model: Thermotron SM32-C Environmental Chamber) was used to undertake tests over a range of different temperatures. Fig. 22 shows the battery test station.

The tests involved repeated discharge and charge tests of the battery, where the discharge time, the battery voltage, the discharge/charge current and the temperature of the battery were recorded.

Furthermore, the battery test station equipment was used to determine the non-linear characteristics of the internal resistance, the self-discharge resistance, the variable resistance R_o and capacitance C_o values of the battery related to open circuit voltage (previously discussed in Section 3.4). The results determined were implemented in the battery model, which characterised these parameters relative to the open circuit voltage VOC. The test data obtained was compared with simulation results and data from the battery manufacturer.

4.1. Battery discharge tests at different rates at standard temperature

To analyse the accuracy of the model over a wide band of discharge rates several discharge tests have been undertaken and the results have been compared with the simulation results. The results of 1 A, 5 A and 20 A discharge tests at standard temperature (25 °C) are shown in Figs. 23–25 compared to simulations suing the author's model. Close correlation between simulation and test results is demonstrated in all cases.

The maximum deviation between simulation results and test data is 0.1 V, which gives a maximum error of less than 1% relative to the experimental data. The error is mainly caused by two main model characteristics:

- VOC versus SOC characteristic;
- I_B versus E_{max} characteristic.

Both are approximations of the true relationships between the battery parameters, and are based on test and manufacturers data. However, the small error experienced can be accepted, seeing the model advantages of the simplifications.

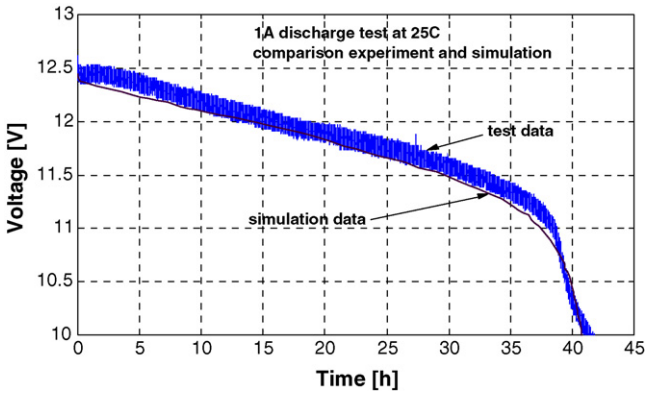

Fig. 23. Voltage–time characteristic 1 A discharge.

4.2. Battery constant 10 A discharge test at different temperatures

As explained in Section 3.5 temperature has a strong influence on the battery performance, and this influence is implemented in the new model by variation of the maximum available capacity/energy of the battery according to Fig. 21. For the chosen application of a stationary fuel cell/battery CHP system the batteries are expected to work in an environment of approximately 15–30 °C. However, for short periods the batteries could

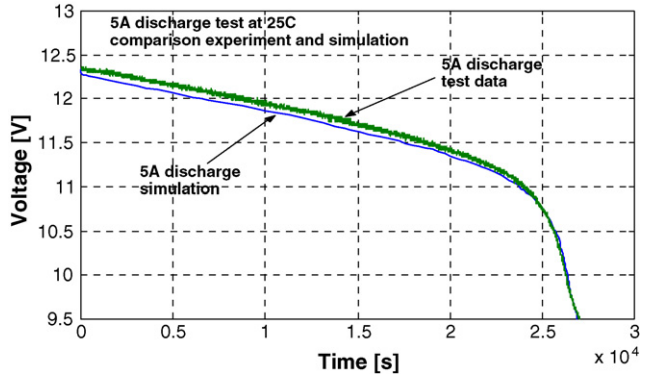

Fig. 24. Voltage–time characteristic 5 A discharge.

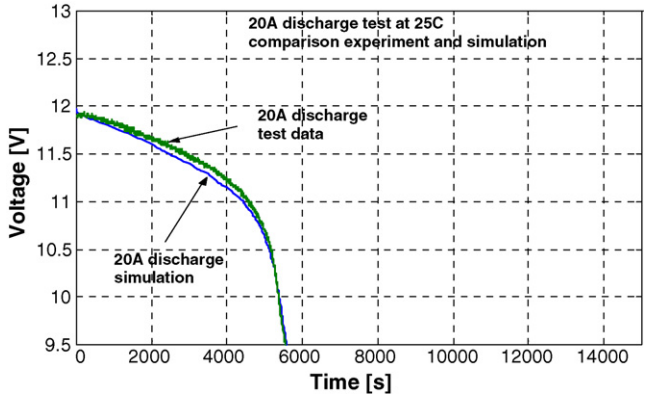

Fig. 25. Voltage–time characteristic 20 A discharge.

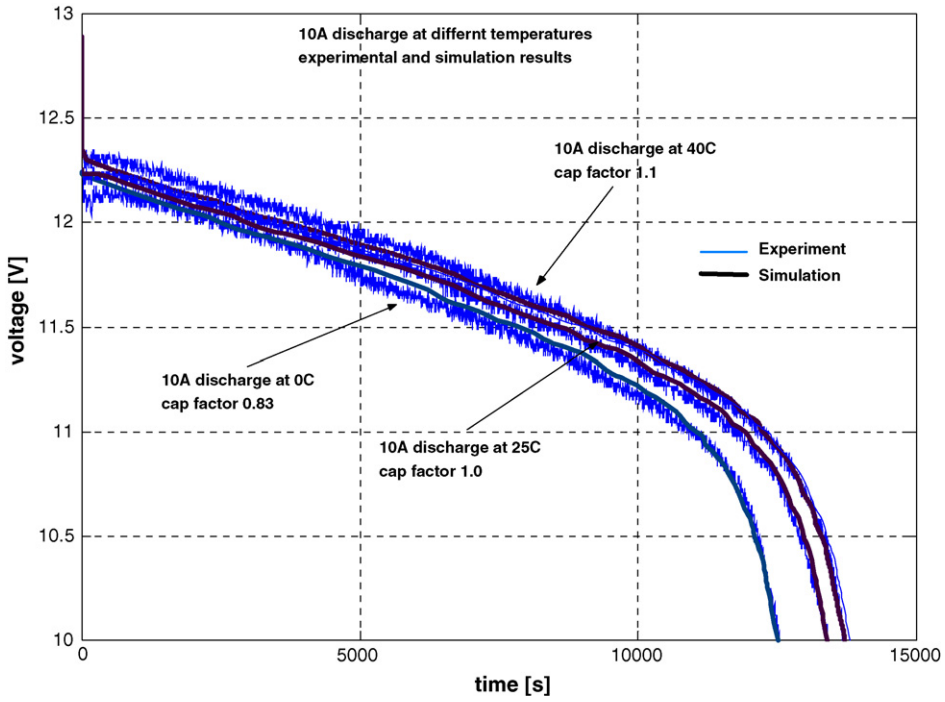

Fig. 26. Voltage–time characteristic 10 A discharge at 0 °C and 40 °C compared to standard condition discharge test at 25 °C.

operate at higher or lower temperatures. To protect the batteries temperatures below 0 °C and higher than 40 °C have to be avoided.

Fig. 26 shows simulation and experimental results for a 10 A discharge test at a temperature of 0 °C and 40 °C compared to a 10 A discharge test at standard conditions (25 °C).

As a result of the temperature corrected maximum energy, the battery model is able to forecast the battery behaviour within the modelled temperature range. As shown in Fig. 26 the model results predict the actual battery discharge relatively accurate.

4.3. Discharge at a typical load profile

The battery model will be used as a part of a domestic scale hybrid fuel cell/battery system model; hence, a discharge test at a predefined, typical load profile was carried out (see current profile in Fig. 28): This load profile was chosen to 'represent' a typical domestic electrical demand at a constant temperature of 25 °C. The discharge current for the single 42 Ah battery varies from 5 A to 50 A during the 1 h test duration. The experimental results have been compared to simulation results from the author's model.

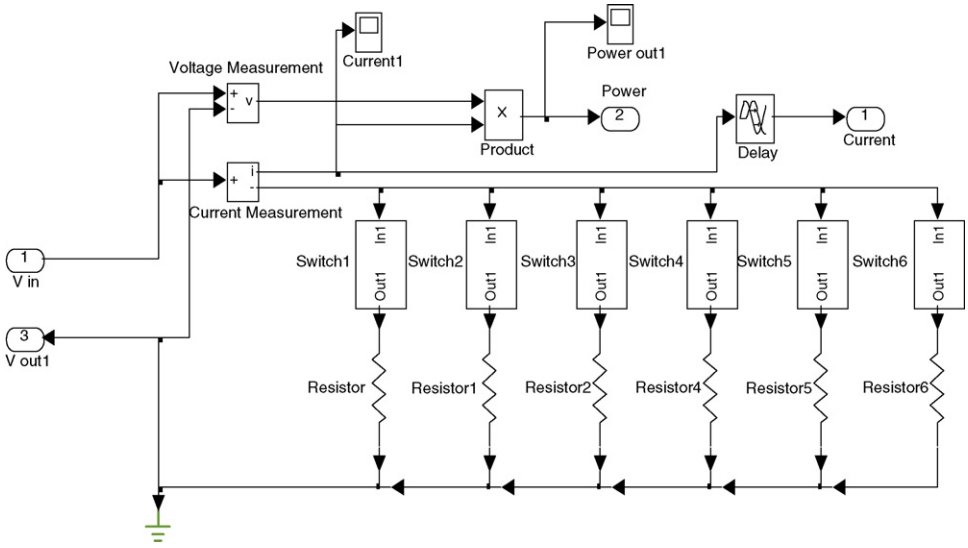

Fig. 27. Load model.

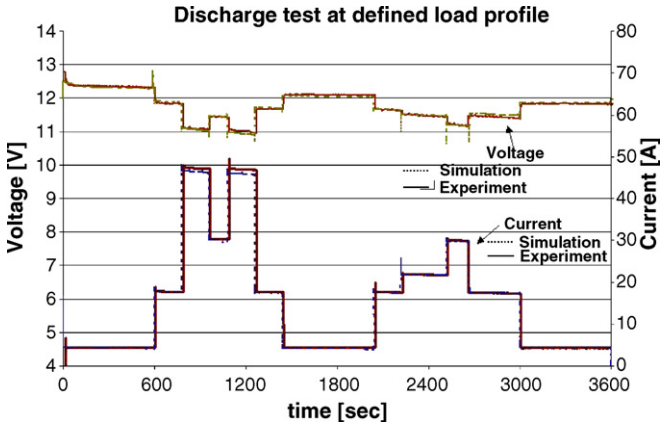

Fig. 28. Load profile discharge test.

The variable load has been modelled as a parallel resistor bank as shown in Fig. 27.

The various resistors can be switched on or off according to the demanded load at the time.

In Fig. 28 the voltage and current characteristics for the test and the simulation are illustrated. It can be seen that the simulation closely matches the test results, supporting the author's claim of a robust and accurate battery model.

4.4. Transient response

To investigate the transient response accuracy of the battery model, load switching tests have been carried out. Figs. 29 and 30 show the current and voltage response for a load switching test from 0 A to 37 A. In both figures the actual test results have been compared with the simulation results.

The results show that the model predicts the battery behaviour accurately. The current spike, paired with a voltage drop, at switching time is caused by the use of a filament light bulb load during the experiment, whereas in the simulation the load is modelled as an ideal resistor bank, hence, no current spike occurs in the simulation.

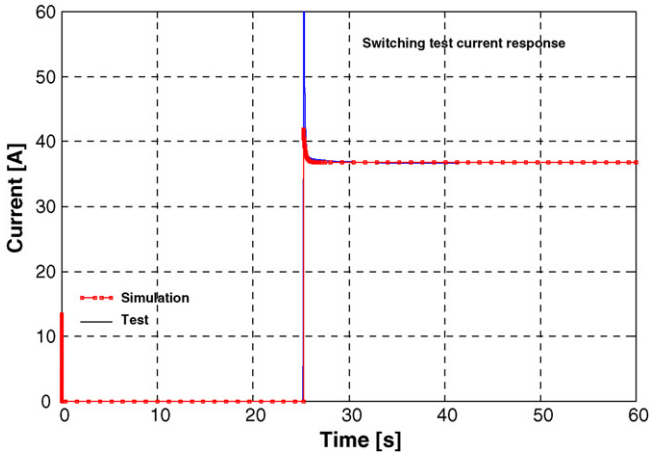

Fig. 29. Switching test current response.

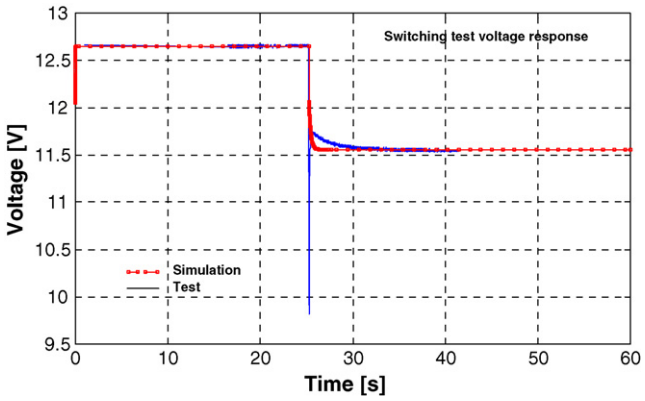

Fig. 30. Switching test voltage response.

5. Discussion of the results and conclusions to the battery model

The mathematical model developed during this work accurately describes the behaviour of a lead acid battery under typical discharge conditions.

By developing and modelling a look-up table to describe the battery state of charge vs. voltage characteristic a simple but accurate method has been developed to model a typically highly non-linear lead acid battery.

The non-linear elements of the battery, such as the internal resistance and the self-discharge resistance have been expressed by functions dependent on the open circuit voltage of the battery. The non-linear functions were determined by experiment and/or taken from the manufacturer's data.

Moreover, a temperature compensation element has been implemented in the model to take account of the temperature effects on the capacity of the battery. Due to the complex electrochemical reactions taking place in the battery the temperature compensation element is only considered to be accurate at present in the range between 0 °C and 40 °C. This limitation is acceptable for the battery buffer/storage device that will be ultimately employed in the Strathclyde University FC system.

As stated before other factors (e.g. cycle history, internal corrosion) influence the battery parameters (e.g. SOC, true capacity) and consequently the battery performance. However, the method suggested provides an easy and practical way to model the battery behaviour for the mentioned application of a fuel cell/battery system.

Switching tests and simulations have shown that the model can be used to simulate different load profiles. The load has been changed over a range of nearly 50 A and the model predicted exactly the voltage and current behaviour of the battery. Additionally the battery's fast transient response to an abrupt load changes has been tested and simulated. Once more the battery response was accurately forecasted by the simulation using the new developed improved battery model.

It remains to be proven that the author's model is also valid for the charging cycle of a lead acid battery. Additionally the model is currently only valid for the specific battery tested and, for accurate modelling of other batteries, the implemented battery

characteristics would have to be developed for each new battery type through tests and/or manufactures data.

This battery model forms part of an overall model of a domestic CHP FC system. This FC system uses a battery buffer/storage consisting of several lead acid batteries, primarily due to cost reasons. Further research will concentrate on battery system modelling, i.e. of several batteries in series, and the development of a monitoring and control algorithm to obtain efficient battery performance and to maintain appropriate battery lifetime.

References

[1] M. Duerr, A. Cruden, Design of an alkaline fuel cell based combined heat and power system for domestic application, in: 13th International Universities Power Engineering Conference, September 2002, Proceedings, vol. 1, pp. 14–18.

[2] K. Klinder, Development and status of plug power/vaillant fuel cell heating, pp. 128–135, in: H. Raak, R. Diethelm (Eds.), The Sulzer Story: From Demonstrators to Commercial Products, pp. 425–433, Proceedings of "The Fuel Cell World" Conference, Lucerne, 1–5 July 2002, Fuel Cells for Power.

[3] M. Newborough, Demand modulation for micro-CHP systems, Power Eng. J. IEE (October) (1999) 257.

[4] G. Cacciola, Low environmental impact energy source: fuel cells, Consiglio Nazionale delle Ricerche (CNR) Report, Italian National Council, Rome (1), vol. 42, 2000.

[5] Up to date price information of batteries from Solarbuzz Inc., 2004, http://www.solarbuzz.com/Batteryprices.htm.

[6] Hawker Energy Products Inc. homepage, 2004, http://www.enersysreservepower.com/catalog.asp.

[7] Battery modelling for HEV simulation, ThermoAnalytics, Inc., 1999, Online publication, http://www.thermoanalytics.com/support/publications/batterymodelsdoc.html.

[8] David Linden, Handbook of Batteries, second ed., 1994, ISBN 0-07-037921-1.

[9] Genesis Application Manual, third ed., Hawker Energy Products Inc., 1997 (Company brochure).

[10] D. Berndt, Maintenance-Free Batteries, John Wiley & Sons, New York, 1997, ISBN 0-86380-143-9.

[11] M. Casacca, Ziyad Salameh, Lead-acid battery storage configurations for improved available capacity, IEEE Trans. Energy Convers. 11 (1) (1996) 139–145.

[12] J.P. Cun, J.N. Fiorina, The experience of a UPS company in advanced battery monitoring, in: Telecommunications Energy Conference, INTELEC'96, October 1996, Proceedings, pp. 646–653.

[13] Battery types and characteristics, ThermoAnalytics, Inc., 1999, Web information http://www.thermoanalytics.com/support/publications/batterytypesdoc.html.

[14] Ziyad M. Salameh, Margaret A. Casacca, A mathematical model for lead-acid batteries, IEEE Trans. Energy Convers. 7 (March (1)) (1992) 93–97.

[15] Margaret A. Casacca, Ziyad M. Salameh, Determination of lead-acid battery capacity via mathematical modelling techniques, IEEE Trans. Energy Convers. 7 (3) (1992) 442–446.

[16] H.L. Chan, D. Sutanto, A new battery model for use with battery energy storage systems and electric vehicles power systems, in: IEEE Power Engineering Society Winter Meeting Conference, vol. 1, NJ, USA, 2000, pp.470–475.

[17] V. Johnson, M. Keyser, Testing, analysis, and validation of a hawker genesis lead-acid battery model in ADVISOR, National Renewable Energy Laboratory, March 1999, http://www.ctts.nrel.gov/analysis/documents/hawker_validation.html.

[18] Genesis Selection Guide, fourth ed., Hawker Energy Products Inc., 2000 (Company brochure).

[19] V.-P. Roan, A. Raman, An approach to incorporating age and temperature effects on performance simulation of electric/hybrid vehicles batteries, IECEC'93 Proceedings of the 28th Intersociety Energy Conversation Engineering Conference, vol. 2, American Chem. Soc., Washington, DC, USA, 1993, pp. 229–237.